

# Impact Testing of Different Materials on Wheels Used in Throwable Unmanned Ground Vehicles

Hamza Sohail<sup>1\*</sup>, Amir Hamza<sup>1</sup>, Nasir Rashid<sup>1</sup>, Muhammad Saad Ali<sup>2</sup>, Taha Ghani<sup>2</sup>

<sup>1,2</sup> Department of Mechatronics Engineering, National University of Sciences and Technology (NUST), CEME, 43701 Rawalpindi, Pakistan

**Abstract.** Throwable Unmanned Ground Vehicles are light weight, small size, easily deployable and impact resistive vehicles mainly used in domestic as well as in military purposes where human life is compromised such as inspection of sewage pipes, and search and rescue operations etc. Main challenge while considering a Throwable UGV is its impact absorption capability which is seen through its material properties. Wheels of Throwable UGV absorb most of the impact without harming the internal structure. To solve this problem a honeycomb structured wheel is designed and simulated in ANSYS Workbench. Vulcanized rubber and Plastic composite PCTPE material wheels were impact tested using explicit dynamic analysis tool in ANSYS workbench. Total deformation, equivalent stress and strain results are tested in ANSYS under impact testing of wheel which is dropped from 10 meter height with velocity of 14m/s in a concrete surface. A plastic composite material PCTPE was 3D-printed and was used in Throwable Unmanned Ground Vehicle.

**Keywords.** *Unmanned Ground Vehicles; Composite Materials; Impact Testing; ANSYS; Land Vehicle; Explicit Dynamic Analysis*

## 1 Introduction

Unmanned Ground Vehicles are bulky in size and difficult to deploy in conditions where human life is compromised. The structure mainly used for UGVs is more military based such as reconnaissance [1, 2], and search and rescue of hostage [3]. Vibrations produced by the UGV also make it less durable for long term uses. Generally, UGVs developed are 4 to 6 wheeled with size up to 60 x 40 x 40 cm. The structure of such UGVs varies from 2 to 4 wheeled. The main components of such UGVs are their wheels which absorb most of the impact. There are two types of structure for wheels honeycomb and flapper design [4, 5]. Both designs work well in their related environments such as rocky environment, flapper wheel works well while honeycomb gives better impact resistance against harsh environments [6, 7]. Honeycomb structure gives better impact resistance due to the space provided between the layers [8, 9]. As most of the problems arise when impact flows through the shaft of Throwable UGV, it may damage or completely destroy the shaft from the inside. For this purpose, wheels should be developed in such a way that impact does not exceed to shaft for reliability of throwable UGV. D-30 rubber material allows the robot to retain its shape and absorb most of the impact after the fall due to its stiffness [7, 8]. When UGV lands on the ground, impact force acts on it, wheel disorient it to prevent damage to internal circuitry. Landing energy is absorbed by the wheel, it retains its shape. Vulcanized rubber [10] is basically usual rubber whose physical properties have been altered using a process called vulcanization. It involves curing the rubber with chemicals like sulfur to make it much more resistant to thermal and atmospheric challenges. Moreover, its tensile strength and elasticity also increases. Nylon is generally a group of synthetic polymers of polyamide [11-12]. Nylon has high tensile strength and has been considered effective as compared to metals in various products due to its anti-corrosion properties and strength.

---

\* Hamza Sohail: [hamza.sohail@ceme.nust.edu.pk](mailto:hamza.sohail@ceme.nust.edu.pk)

Polyurethane is an organic polymer in which different organic units are linked through urethane molecules. It provides excellent heat resistance and works satisfactorily under pressure therefore it was considered an option for wheel manufacture [13-16]. It is used in sand flee robot [17-22], a robot which uses actuation to jump for at a certain height [23-26]. Thermoplastic polyurethane (TPU) [27] is generally a variant of polyurethane in which it undergoes specific processes to make it thermal resistant. TPU is durable, biodegradable and recyclable. Thermoplastic Elastomers (TPE) [28-30] are a mixture of polymers having both thermoplastic and elastomeric properties making it both hard and impact resistant like plastics and soft and impact absorbent like rubber. Design requirement includes weight, size, and material properties. Carbon Fiber wheels are light weight and impact resistive with high ultimate tensile strength [31]. It was first analyzed by navy in which full Throwable UGV consisted of carbon fiber body along with wheels. It was manufactured to withstand in marine environment. PCTPE material [8] was considered on the basis of its light weight; easily 3D printed and has ultimate tensile strength of 34 MPa [8]. Manufacturing of wheels can be done in two ways 3D printing and molding process. 3D printing process is flexible as compared to molding process as 3D printing is better for small batch, complex parts in which designs are complex. On the other hand for designs with lesser complexity can be manufactured by molding processes. The main goal of the research is to test different materials for the wheels of UGVs to make them throwable and lightweight.

## 2 Methodology

To design a wheel for Throwable Unmanned Ground Vehicle, the main components that are considered are their material properties and energy that wheel is absorbing on impact. A free falling wheel can be modeled using its impulse response which can be seen as change in momentum that a wheel undergo is equals to the impact force times the duration of impact [33].

$$\Delta mv = \int F(t)dt \quad (1)$$

‘m’ is the mass of wheel, ‘v’ is the velocity before and after the impact, and ‘F(t)’ is the impact force during the time of impact. The illustration of impulse response of a free falling perfectly elastic wheel without any energy loss is shown in figure 1(a) while non-ideal behavior is shown in figure 1(b). It shows how a wheel is fallen from a height. Before hitting the ground it has the velocity of ‘v<sub>1</sub>’. As the wheel hits the ground it bounces back a height ‘h<sub>2</sub>’ with a velocity of v<sub>2</sub> to release the amount of energy which was absorbed on hitting the ground.

$$v_i = \sqrt{2gh_i} \quad (2)$$

v<sub>i</sub> is the free falling velocity of a wheel. ‘i’ shows the velocity at different instances as shown in figure 1(b). Figure 1(a) shows E is the point of impact. Here on point E wheel is in compressed state and does feel the stress on it. Yellow color represents that a shock with the speed of sound in solid flows through it. At point F ball is fully in a stressed state as it is fully energized by the impact force and kinetic energy has been fully transferred into potential energy. We can safely assume that at point F velocity is zero.

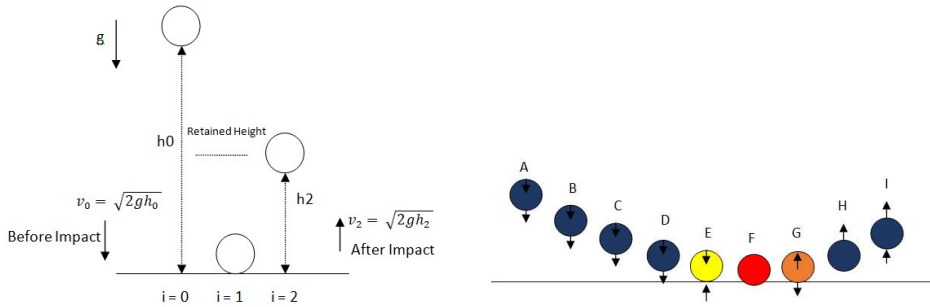


Figure 1(a) Impulse response of perfectly elastic wheel, (b) Before and after impact response

Material properties play a significant role in impact absorption, its young's modulus and density as they are related with the speed of sound in solid during the time of absorption. The square root ratio of young's modulus to density of a wheel is known as speed of sound in solids ' $\sigma$ '.

$$\sigma = \sqrt{\frac{E}{\rho}} \tag{3}$$

Duration of impact is the time taken by the body before and after the collision. Since energy is absorbed by the wheel during the time of collision and after that it is released. The duration of impact is defined as the ratio of two times diameter 'D' of wheel to speed of sound in solid.

$$\Delta t = \frac{2D}{\sigma} \tag{4}$$

Stress acted on the wheel during the time of collision can be represented as the ratio of impact force acted on the wheel during the time of impact by area of impact. Since we are considering wheel as perfectly elastic we can also assume it as a spring. Hence the spring coefficient 'S' is  $S = \frac{AE}{D}$  where A is the area of impact, D is diameter of wheel and E is young's modulus.

$$Stress = \frac{F}{A} \tag{5}$$

To make a low weight wheel honeycomb structure [32] is considered as it is helpful in circumstances where shaft of the wheel is compromised after the impact. Most of the impact absorbs by the wheel move from bottom to top and it greatly affects the internal structure as well as shaft. To avoid such impact honeycomb is designed so that impact can be spread across the wheel instead of focused on shaft. The structure in figure 2(a) consists of two vertical series of quadrilateral holes made in circular sequence, with 20 holes on the upper series and 10 holes on the inner series of the wheel body. The quadrilateral designs are curves around the corners to disperse the stress which is caused by the fall for a height. The outer side of the wheels is curved, with depth increasing as the design traverses near to the center. This was done to assist the easy bending of the outer portion while resisting the bending as the impact reaches the inner section of the wheel, doing so should decrease the impact reaching the shaft, and through the shaft, to the body. Figure 2(b) is designed to be semi-flexible; hence it has Plasticized Co-polyimide Thermoplastic Elastomer (PCTPE) material-based design. The outer rim has been made thin to enable easy dispersion of force due to impact, by easy bending of the outer rim more strands of the wheel's inner design

are engaged hence dividing the force among the middle portion of the wheel and minimizing the force reaching the center of the wheel, and through the center to the shaft of the robot. Every other column of the wheel has comparatively larger width than the other to provide support to the structure of the wheel.

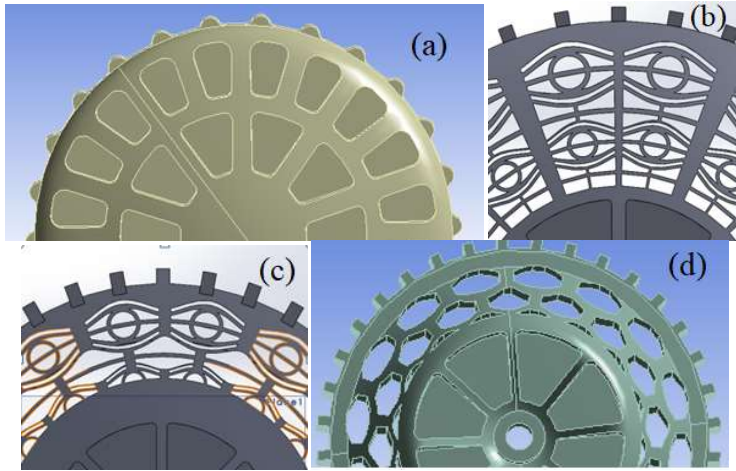


Figure 2 (a) Honeycomb conventional structure, (b) Semi-flexible design1, (c) Semi-flexible design2, (d) Final Design

As figure 2(b) shows, the design of the middle section is made to bend and disperse much force of the impact. The design consists of four vertical series. The series, first to the top, and the third series consists of improved honeycomb structure which allows more bending than conventional honeycomb design. The inner portion of the honeycomb consists of a circular support which provides structural support to the honeycomb structure. The second vertical series is also an enhanced honeycomb design which provides vertical support to the structure to prevent bending to increase out of proportion. The fourth vertical series is an alternate pentagon design which provides support to the thin columns hence improving the structure of the wheel. Figure 2(b) shows the inner most section of the wheel consists of curved quadrilateral holes with 5mm plain sheet closing the other end. This was done to divert the remaining force to the outer section of the shaft. The columns in-between the quadrilateral provide support to the structure of the wheels. As in figure 2(c), the middle and the center design of the wheel has been altered. In the middle section, three horizontal series have been designed. The first series is the same as that of figure 2(c). In the second series, the columns which were at the center of the hexagonal structure in figure 2(c) have been removed from within the hexagons. This was done to increase the controlled bending of the second series layer. The columns which were thin in figure 2(c) were made wider to the width of the larger columns to provide support to the second layer. The third series is same as the first series, but it is the upper half portion of it. The place of the fourth series has been filled up to provide space for the in-mounting of the body on the other side of wheel. This is presented in figure 2(c). This space provides the mounting of the body of robot inside the structure of the wheels. When the wheels bend due to the force of impact, the force is transferred to the body instead of the shaft, and through the shaft, to the inner body circuitry. Apart from these variations, the rest of the design is the same as that of figure 2(b).

Figure 2(d) is a simplified design based on figure 2(c). It was designed to simplify the design of figure 2(c). Fig. 2(c) was a satisfactory design, but it is comparatively complex to be 3d printed considering the primordial expertise of the local 3d printing services. The intricate details of figure 2(c) are difficult to print as they require printing of fine details. So, in figure 2(d), these intricate details were made simpler in order to provide ease of printing. The design was developed by 3D print as shown in figure 2(d) and impact analysis was done on it.

The material properties of PCTPE and vulcanized rubber show that densities of both are almost same. Young’s Modulus of PCTPE is greater since it is stiffer than vulcanized rubber. PCTPE is semi-flexible material while vulcanized rubber is flexible. Table 1 shows complete material properties of PCTPE and vulcanized rubber

Table 1 Material Properties of PCTPE and vulcanized material

Material	Density Kg/m <sup>3</sup>	Young’s Modulus MPa	Bulk Modulus MPa	Shear Modulus MPa	Poisson’s Ratio	Ultimate Tensile Strength MPa	Elongation at break
PCTPE	1113	75.0	56.0	29.3	0.28	34.8	497%
Vulcanized Rubber	950	16.3	138	55.0	0.48	28.0	100-800%

### 3 Results and Discussions

Analysis is done on final design selected in figure 2(d). Explicit dynamic analysis [30] on ANSYS workbench is used to get total deformation, equivalent stress and strain of PCTPE and vulcanized rubber material. Wheel is undergone impact testing with velocity of 14m/s. It is dropped from a height of 10 meters in a concrete surface. The ultimate tensile strength of PCTPE is 34 MPa and 28MPa of vulcanized rubber [34, 35]. This suggests from the number which will be feasible. But the main challenge here is to identify if other composite materials that are light weight and easily made by 3D-printing are sustainable for Throwable Unmanned Ground Vehicle. To solve this problem analysis is done. Meshing is done first. Size function is set to adaptive, high smoothing, slow transition, coarse span angle center and 1.218e-06m minimum edge length is set for smooth analysis. Number of nodes in mesh are 13211 and number of elements generated are 51135. There are only three factors that are needed total deformation, equivalent stress and strain. After analysis the results of total deformation are shown in figure 3. Both wheels have slight deformation due to their flexibility. PCTPE material has total deformation of 16.7 mm while deformation of vulcanized rubber is 13.9 mm.

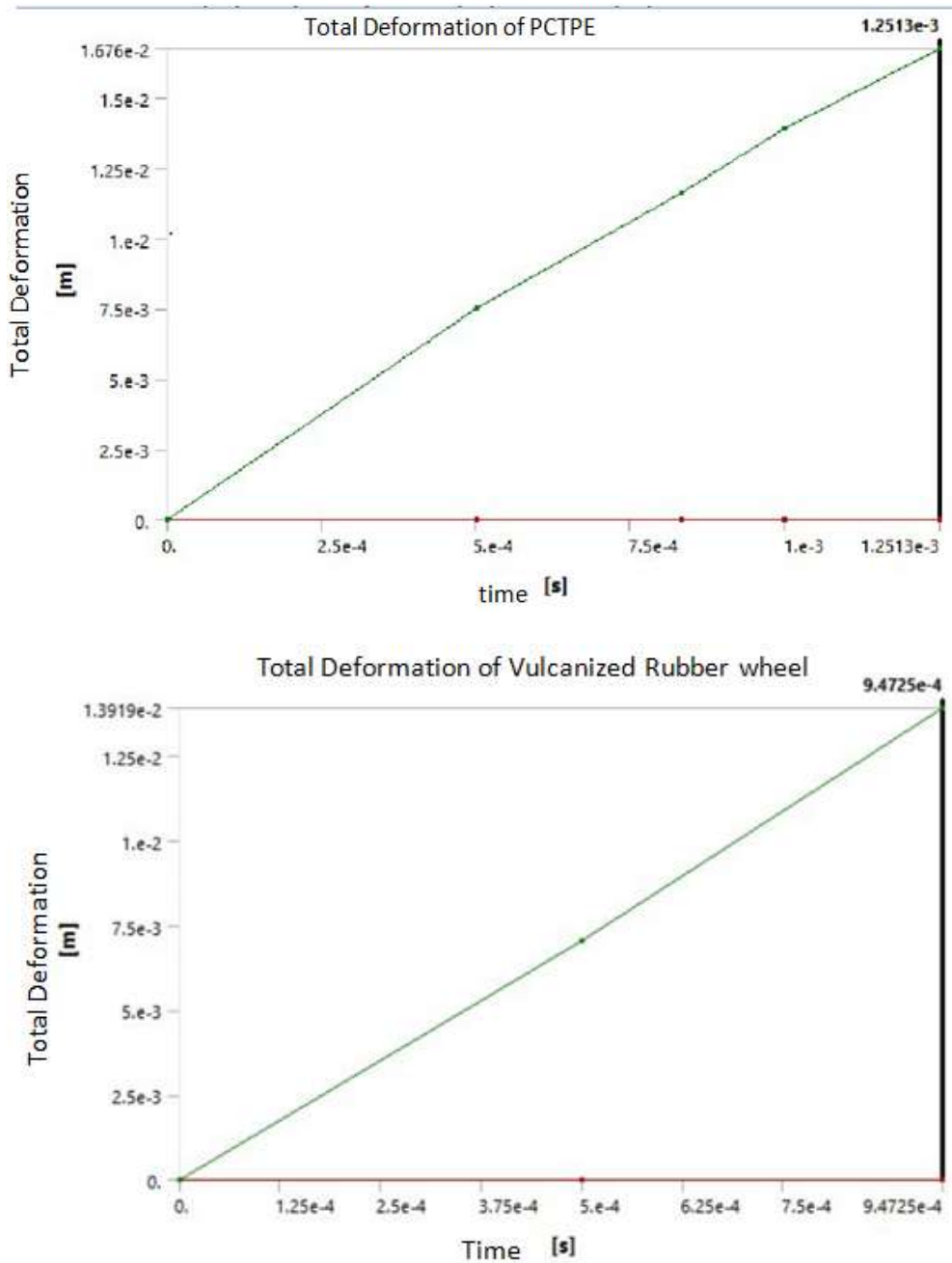


Figure 3 Total Deformation (a) PCTPE, (b) Vulcanized Rubber

Figure 4 shows von-mises stress on wheels of PCTPE and vulcanized rubber material. Maximum stress that PCTPE material has is 29.6 MPa which is slightly lower as compared to its ultimate tensile strength which is 34 MPa. Similarly, in vulcanized rubber wheel that can bear stress of 6.5 MPa which is lower than its ultimate tensile strength that is 28MPa which is shown in table 1.

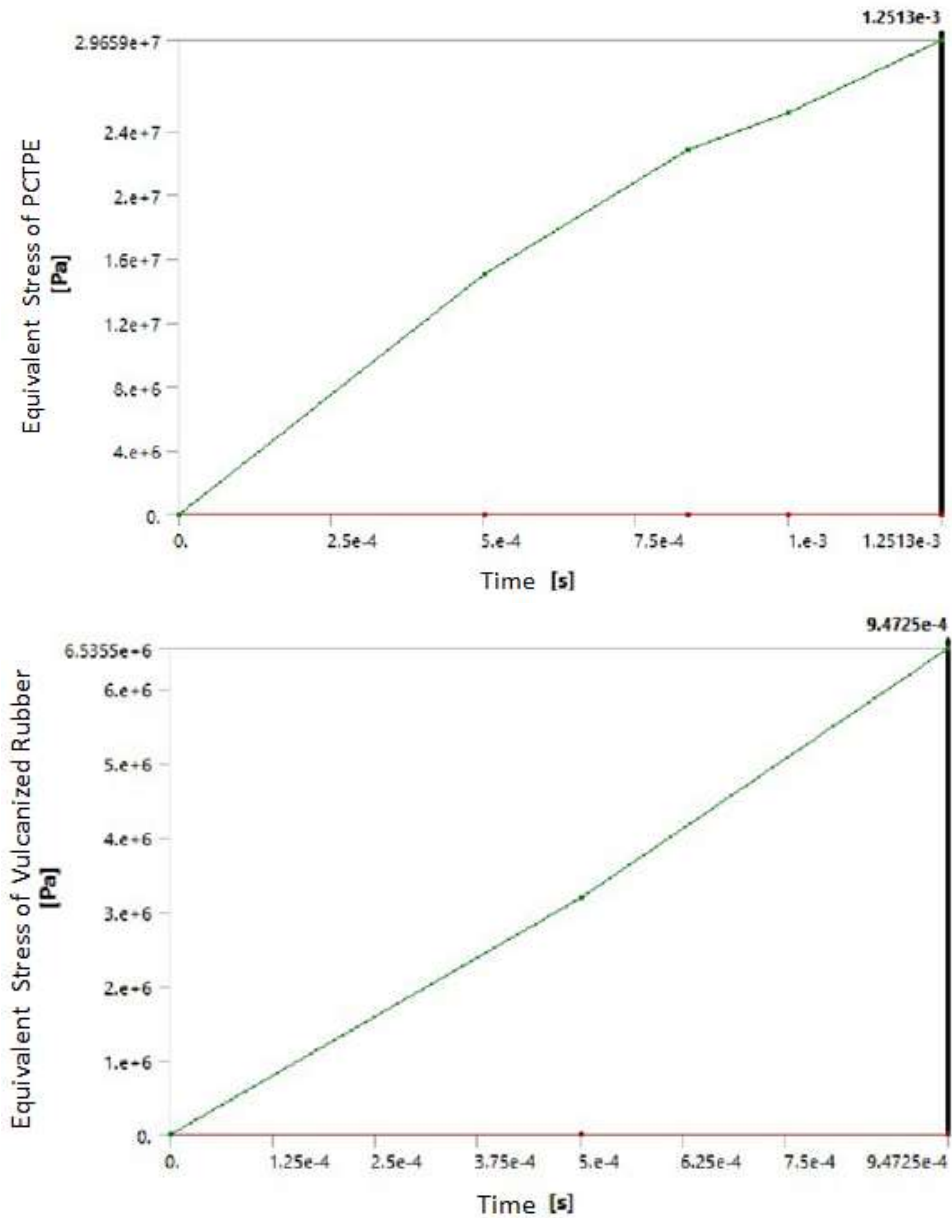


Figure 4 Equivalent Stress (a) PCTPE, (b) Vulcanized Rubber

Figure 5 shows equivalent stress of both PCTPE and vulcanized rubber wheel. PCTPE shows stress that is distributed across the wheel. While in vulcanized rubber wheel stress is distributed in lower surface of the wheel. The concentration of stress on vulcanized rubber wheel is higher on the surface of impact.

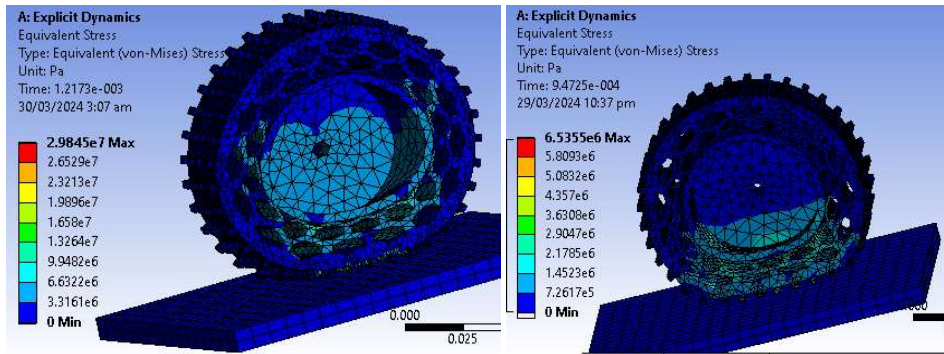
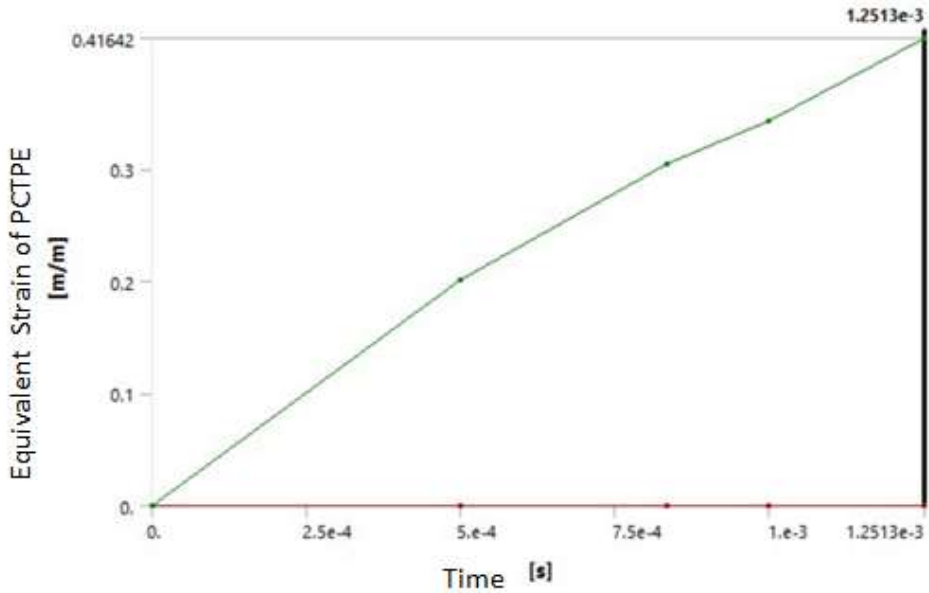


Figure 5 Equivalent Stress ANSYS (a) PCTPE, (b) Vulcanized Rubber

Equivalent strain of PCTPE vs vulcanized rubber is shown in figure 6. It shows 41% and 40% elongation of PCTPE and vulcanized rubber with respect to time. As shown in table 1 PCTPE breaks at elongation at 497% while vulcanized rubber wheel breaks at elongation of 100 to 800% depending on the condition. In the case above it is only elongated to 40%.



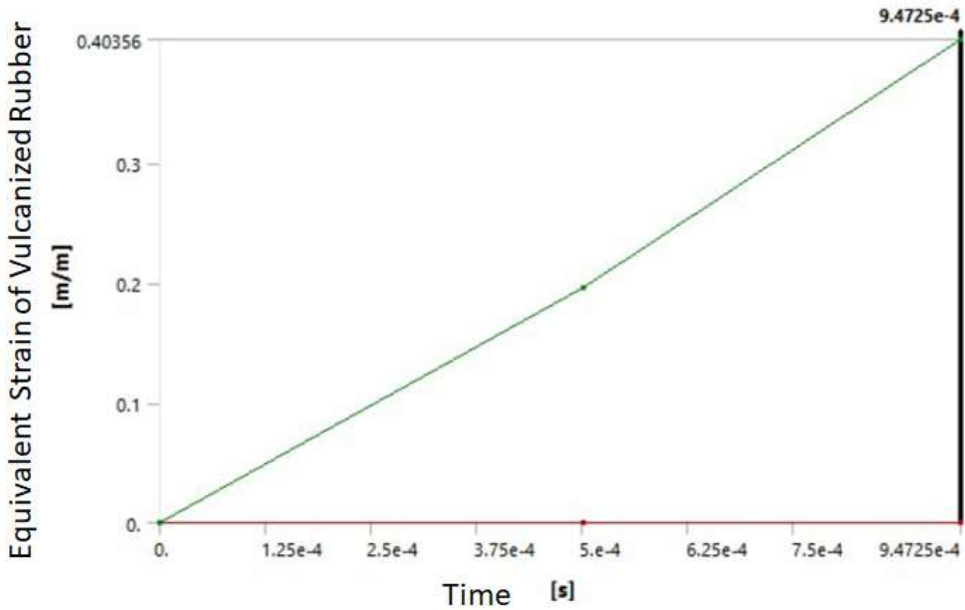


Figure 6 Equivalent Strain (a) PCTPE, (b) Vulcanized Rubber

Stress-strain curve can be compared by using figure 4, 6. Here we can validate the results by simply dividing the stress to strain. Maximum stress that is occurring in PCTPE wheel is 29.6 MPa and strain is 0.41 m/m. If we divide the two we get young’s modulus of around 72.1 MPa which is closer to 75 MPa. The error is 3.86% while in case of vulcanized rubber the error is 0.74%. The values are shown in table 2.

Table 2 Validation of Results using young’s modulus			
Materials	Young’s Modulus	Young’s Modulus	% error
	Original	Impact testing	
PCTPE	75.0 MPa	72.16 MPa	3.86%
Vulcanized Rubber	16.3 MPa	16.18 MPa	0.74%

## 4 Conclusions

- The results were analyzed in ANSYS workbench under explicit dynamic analysis in which wheels with different materials were tested. In ANSYS, wheels were fallen from height of 10 meters having 14m/s velocity.
- Results suggest that both PCTPE and vulcanized rubber material wheels can withstand the fall of 10 meters and can be used in the development of Throwable Unmanned Ground Vehicle.
- The main reason for choosing PCTPE over vulcanized rubber material is the manufacturing process. PCTPE wheels are easily available and can be 3D printed while vulcanized rubber wheel are manufactured by molding process. The design shown in figure 2(d) is 3D printed with PCTPE material and is tested under static loading conditions.

- Figure 7 shows the manufactured wheel in which vulcanized rubber coating is used to improve its efficiency. Adhesive material is used to attach the layer of vulcanized rubber on PCTPE wheel. Hardener and resin is used for this purpose.



Figure 7 Developed wheel for Throwable Unmanned Ground Vehicle

## References:

1. Hougen, D.F., Benjaafar, S., Bonney, J.C., Budenske, J.R., Dvorak, M., Gini, M., French, H., Krantz, D.G., Li, P.Y., Malver, F. and Nelson, B., 2000, April. A miniature robotic system for reconnaissance and surveillance. In *Proceedings 2000 ICRA. Millennium Conference. IEEE International Conference on Robotics and Automation. Symposia Proceedings (Cat. No. 00CH37065)* (Vol. 1, pp. 501-507). IEEE.
2. Stoeter, S.A., Rybski, P.E., Stubbs, K.N., McMillen, C.P., Gini, M., Hougen, D.F. and Papanikolopoulos, N., 2002. A robot team for surveillance tasks: Design and architecture. *Robotics and Autonomous Systems*, 40(2-3), pp.173-183.
3. Zhang, L., Huang, Q., Zhang, W., Li, Y., Huang, Y., Li, H. and Wu, L., 2011, August. Design and realization for throwable semi-autonomous reconnaissance robot. In *2011 IEEE International Conference on Automation and Logistics (ICAL)* (pp. 6-11). IEEE.
4. Zhang, L., Huang, Q., Huang, Y., Li, Y., Sang, W. and Wu, L., 2011, June. Mechanical designs and control system of throwable miniature reconnaissance robot. In *2011 IEEE International Conference on Information and Automation* (pp. 431-436). IEEE.
5. Chemel, B., Mutschler, E. and Schempf, H., 1999, May. Cyclops: Miniature robotic reconnaissance system. In *Proceedings 1999 IEEE International Conference on Robotics and Automation (Cat. No. 99CH36288C)* (Vol. 3, pp. 2298-2302). IEEE.
6. Stoeter, S.A., Rybski, P.E., Stubbs, K.N., McMillen, C.P., Gini, M., Hougen, D.F. and Papanikolopoulos, N., 2002. A robot team for surveillance tasks: Design and architecture. *Robotics and Autonomous Systems*, 40(2-3), pp.173-183.
7. Zhang, L., Huang, Q., Li, Y., Gao, J., Li, H. and Wu, L., 2012, August. Research and development of throwable miniature reconnaissance robot. In *2012 IEEE international conference on mechatronics and automation* (pp. 1254-1259). IEEE.
8. Sohail, H., Hamza, A., Rashid, N., Ali, M.S. and Ghani, T., 2023, March. Design and Analysis of Throwable Unmanned Ground Vehicle. In *2023 International Conference on Robotics and Automation in Industry (ICRAI)* (pp. 1-6). IEEE.
9. Li, Y., Huang, Q., Gao, J., Zhang, L. and Tian, Y., 2012, July. A novel semi-autonomous throwbot for reconnaissance application. In *Proceedings of the 10th World Congress on Intelligent Control and Automation* (pp. 3822-3827). IEEE.
10. Liu, Q., Zhang, Y. and Xu, H., 2008. Properties of vulcanized rubber nanocomposites filled with nanokaolin and precipitated silica. *Applied Clay Science*, 42(1-2), pp.232-237.

11. Shakiba, M., Rezvani Ghomi, E., Khosravi, F., Jouybar, S., Bigham, A., Zare, M., Abdouss, M., Moaref, R. and Ramakrishna, S., 2021. Nylon—A material introduction and overview for biomedical applications. *Polymers for advanced technologies*, 32(9), pp.3368-3383.
12. Kojima, Y., Usuki, A., Kawasumi, M., Okada, A., Fukushima, Y., Kurauchi, T. and Kamigaito, O., 1993. Mechanical properties of nylon 6-clay hybrid. *Journal of materials research*, 8(5), pp.1185-1189.
13. Zhao, J., Yan, W., Xi, N., Mutka, M.W. and Xiao, L., 2014, May. A miniature 25 grams running and jumping robot. In *2014 IEEE International Conference on Robotics and Automation (ICRA)* (pp. 5115-5120). IEEE.
14. Zhao, J., Xu, J., Gao, B., Xi, N., Cintron, F.J., Mutka, M.W. and Xiao, L., 2013. MSU jumper: A single-motor-actuated miniature steerable jumping robot. *IEEE Transactions on Robotics*, 29(3), pp.602-614.
15. Cintron, F.J., Pongaliur, K., Mutka, M.W., Xiao, L., Zhao, J. and Xi, N., 2012. Leveraging height in a jumping sensor network to extend network coverage. *IEEE transactions on wireless communications*, 11(5), pp.1840-1849.
16. Zhang, J., Song, G., Li, Z., Qiao, G., Sun, H. and Song, A., 2012, October. Self-righting, steering and takeoff angle adjusting for a jumping robot. In *2012 IEEE/RSJ International Conference on Intelligent Robots and Systems* (pp. 2089-2094). IEEE.
17. Li, F., Liu, W., Fu, X., Bonsignori, G., Scarfogliero, U., Stefanini, C. and Dario, P., 2012. Jumping like an insect: Design and dynamic optimization of a jumping mini robot based on biomimetic inspiration. *Mechatronics*, 22(2), pp.167-176.
18. Kovač, M., Schlegel, M., Zufferey, J.C. and Floreano, D., 2010. Steerable miniature jumping robot. *Autonomous Robots*, 28, pp.295-306..
19. Woodward, M.A. and Sitti, M., 2011, September. Design of a miniature integrated multi-modal jumping and gliding robot. In *2011 IEEE/RSJ International Conference on Intelligent Robots and Systems* (pp. 556-561). IEEE.
20. Zhao, J., Yang, R., Xi, N., Gao, B., Fan, X., Mutka, M. and Xiao, L., 2009. Development of a self-stabilization miniature jumping robot. In *Proc. IEEE/RSJ Int. Conf. Intell. Robots Syst* (pp. 2217-2222).
21. Zhao, J., Xi, N., Gao, B., Mutka, M.W. and Xiao, L., 2010, October. Design and testing of a controllable miniature jumping robot. In *2010 IEEE/RSJ International Conference on Intelligent Robots and Systems* (pp. 3346-3351). IEEE.
22. Zhao, J., Xi, N., Gao, B., Mutka, M.W. and Xiao, L., 2011, May. Development of a controllable and continuous jumping robot. In *2011 IEEE International Conference on Robotics and Automation* (pp. 4614-4619). IEEE.
23. Yamada, A., Mameda, H., Mochiyama, H. and Fujimoto, H., 2010, October. A compact jumping robot utilizing snap-through buckling with bend and twist. In *2010 IEEE/RSJ International Conference on Intelligent Robots and Systems* (pp. 389-394). IEEE.
24. Noh, M., Kim, S.W., An, S., Koh, J.S. and Cho, K.J., 2012. Flea-inspired catapult mechanism for miniature jumping robots. *IEEE transactions on robotics*, 28(5), pp.1007-1018.

25. Tanaka, T. and Hirose, S., 2008, September. Development of leg-wheel hybrid quadruped "AirHopper" design of powerful light-weight leg with wheel. In *2008 IEEE/RSJ International Conference on Intelligent Robots and Systems* (pp. 3890-3895). IEEE.
26. Kim, D.H., Lee, J.H., Kim, I., Noh, S.H. and Oho, S.K., 2008. Mechanism, control, and visual management of a jumping robot. *Mechatronics*, *18*(10), pp.591-600.
27. Herrera, M., Matuschek, G. and Kettrup, A., 2002. Thermal degradation of thermoplastic polyurethane elastomers (TPU) based on MDI. *Polymer degradation and stability*, *78*(2), pp.323-331.
28. Abdou-Sabet, S., Puydak, R.C. and Rader, C.P., 1996. Dynamically vulcanized thermoplastic elastomers. *Rubber chemistry and technology*, *69*(3), pp.476-494.
29. Panda, H.S. and Jagadeesha, T., 2021. Impact analysis of rifle bullet on corrugated sandwich panel structures for defense applications. *Materials Today: Proceedings*, *46*, pp.8444-8449.
30. Chang, C.L. and Yang, S.H., 2008. Finite element simulation of wheel impact test. *Journal of Achievements in Materials and Manufacturing Engineering*, *28*(2), pp.167-170.
31. Nguyen, H.G. and Castelli, R., 2014, June. Development and evaluation of the Stingray, an amphibious maritime interdiction operations unmanned ground vehicle. In *Unmanned Systems Technology XVI* (Vol. 9084, pp. 213-226). SPIE.
32. Gong, X., Ren, C., Liu, Y., Sun, J. and Xie, F., 2022. Impact response of the honeycomb sandwich structure with different Poisson's ratios. *Materials*, *15*(19), p.6982.
33. Li, H., Chen, W. and Hao, H., 2020. Factors influencing impact force profile and measurement accuracy in drop weight impact tests. *International Journal of Impact Engineering*, *145*, p.103688.
34. Makuuchi, K., Yoshii, F. and Gunewardena, J.A.G.S.G., 1995. Radiation vulcanization of NR latex with low energy electron beams. *Radiation Physics and Chemistry*, *46*(4-6), pp.979-982.
35. Sahu, S.K. and Sreekanth, P.R., 2022. Experimental investigation of in-plane compressive and damping behavior anisotropic graded honeycomb structure. *Arabian Journal for Science and Engineering*, *47*(12), pp.15741-15753.